mmol) in Et_2O (30 mL)–THF (2 mL). After 6.5 h at 22 °C the suspension was cooled to 5 °C and 1 N H_3PO_4 (20 mL) was added carefully. The Et_2O phase was separated and the aqueous phase was extracted with Et_2O (3 × 20 mL). After drying, solvent was removed in vacuo to obtain **13a** (94% yield),[13a] which could be recrystallized from EtOAc/hexane to yield a fluffy white solid (69%).

N^{α}-(Benzyloxycarbonyl)-β-bromo-L-alanine (14a). Magnesium bromide etherate was prepared by dropwise addition of distilled (over P_2O_5) Br_2(1) (1.0 mL, 19 mmol) to a suspension of excess Mg filings (1.0 g, 41 mmol) in Et_2O (20 mL) at 0 °C in a flask equipped with an acetone/CO_2(s) condensor. Following the disappearance of Br_2, dry benzene (5 mL) was added, and an aliquot (2 mL, 1.6 mmol $MgBr_2$) of this solution was added to Z-L-serine β-lactone (**3a**) (100 mg, 0.45 mmol) in Et_2O (20 mL)–THF (2 mL). After 5 min, the L-isomer of **14a** was isolated as outlined for **13a** (yield 99%, 67% recrystallized from CH_2Cl_2/hexane).[30] The D-antipode was obtained from Z-D-serine β-lactone (**3a**): mp 70–71 °C (L), 68–69.5 °C (D); $[\alpha]^{22}_D$ +14.2° (L), −14.2° (*D*), (c 1, MeOH); IR (KBr disk) 3390 (s), 1730 (vs), 1648 (s), 1525 (s), 1433 (m), 1290 (m), 1180 (m), 1072 (m), 992 (m), 756 (m), 698 (m) cm^{-1}; ^1H NMR (80 MHz, CD_2Cl_2) δ 8.63 (br s, 1 H), 7.38 (s, 5 H), 5.75 (br s, 1 H), 5.15 (s, 2 H), 4.87 (m, 1 H), 3.83 (m, 2 H). Anal. ($C_{11}H_{12}BrNO_4$) C, H, N, Br. POSFAB-MS (glycerol): MH^+ 302 (17%), $(M+2)H^+$ 304 (17%).

Acknowledgment. We are grateful to the National Institutes of Health (GM 29826), the Natural Sciences and Engineering Research Council of Canada, and the Alberta Heritage Foundation for Medical Research for financial support.

Registry No. DL-**2a**, 2768-56-1; L-**2a**, 1145-80-8; D-**2a**, 6081-61-4; L-**2b**, 3262-72-4; DL-**3a**, 98672-78-7; L-**3a**, 26054-60-4; D-**3a**, 98632-91-8; L-**3b**, 98541-64-1; L-**4a**, 70897-15-3; D-**5a**, 62234-37-1; L-**5b**, 76387-70-7; L-**6a**, 98541-65-2; D-**7a**, 98541-66-3; D-**8a**, 98632-92-9; L-**9a**, 19645-29-5; DL-**10a**, 14464-15-4; D-**11a**, 22911-80-4; D-**12a**, 98541-67-4; DL-**12a**, 98541-68-5; D-**13a**, 73491-16-4; L-**14a**, 98541-69-6; D-**14a**, 98541-70-9; Me_3N, 75-50-3; $HSCH_2CH_2NH_2$·HCl, 156-57-0; NaOAc, 127-09-3; NaOMe, 121-41-4; $PhCH_2SH$, 100-53-8; pyrazole, 288-13-1; thiourea, 62-56-6; (*Z*)-dehydroalanine methyl ester, 21149-17-7.

Role of Agostic Interaction in β-Elimination of Pd and Ni Complexes. An ab Initio MO Study

Nobuaki Koga, Shigeru Obara,[1a] Kazuo Kitaura,[1b] and Keiji Morokuma*

Contribution from the Institute for Molecular Science, Myodaiji, Okazaki 444, Japan, the Department of Chemistry, Kyoto University, Kyoto 606, Japan, and the Department of Chemistry, Osaka City University, Osaka 508, Japan. *Received December 10, 1984*

Abstract: We optimized the geometries of $Pd(C_2H_5)(H)(PH_3)$ (**1**), $Pd(H)_2(C_2H_4)(PH_3)$ (**2**), and the transition state between them and calculated the barriers for β-elimination and its reverse, insertion reaction. **1** has a distorted ethyl group, which is a sign of agostic interaction, a direct CH···M interaction. The low-energy barrier for **1** → **2** β-elimination is located in the direction of a direct extension of agostic interaction. Similar calculations for $Pd(CH_2CHF_2)(H)(PH_3)$ (**3**) and $Ni(C_2H_5)(H)(PH_3)$ (**4**), their transition states, and β-elimination products show that **3** and **4** have much weaker agostic interaction and higher barriers. Factors determining the differences among these systems in the structure and barrier height have been discussed in detail. Though it may not be easy to detect experimentally, the present study strongly suggests that in unstable reactive intermediates an agostic interaction may be taking place more commonly than has been suspected and that it is responsible to facile β-elimination.

Intramolecular interaction between a rather inert CH bond and the central metal in transition-metal complexes, called an agostic interaction, has attracted much attention lately, since the interaction is considered to be important in such reactions as α-elimination, β-elimination, orthometalation, and related reactions.[2] The interaction has been observed by the determination of crystal structures by X-ray and neutron diffraction methods. Complexes in which the central transition metal interacts with a CH bond exhibit characteristic structural features: the CH···M distance is shorter than the sum of van der Waals radii and the interacting CH bond distance is longer than the normal CH bond. NMR and IR spectra have also indicated the existence of such an interaction in some complexes. The driving force for the interaction has been considered to be the inclination to satisfy the 18-electron rule, since all the cases involve electron-deficient metals.

Recently, we have reported the first theoretical evidence for CH···M interaction found in ab initio molecular orbital calculations.[3] Our theoretical studies on $Ti(C_2H_5)(Cl)_2(H)(PH_3)_2$ (**5**) have reproduced essential structural features which have been experimentally observed in $Ti(C_2H_5)(Cl)_3(dmpe)$ (dmpe = (dimethylphosphino)ethane) by X-ray structural analysis.[4a] The complex **5** has been calculated to have the Ti–C–C angle of 89°,

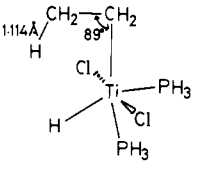

5

much smaller than the tetrahedral angle, and a CH^{β} bond distance of 1.114 Å, 0.03 Å longer than the normal CH bond. The optimized structure of $Ti(CH_3)(Cl)_3(PH_3)_2$ (**6**) also indicates the existence of agostic interaction between the methyl α-hydrogen and the metal. The recent neutron diffraction study gives the Ti–C–H angle of 94°, much closer to our theoretically predicted value of 100° than the earlier X-ray result of 69°.[4b,c,5] These

* Address correspondence to this author at the Institute for Molecular Science.

(1) (a) Kyoto University. (b) Osaka City University.
(2) Brookhart, M.; Green, M. L. H. *J. Organomet. Chem.* **1983**, *250*, 395 and references cited therein.
(3) (a) Koga, N.; Obara, S.; Morokuma, K. *J. Am. Chem. Soc.* **1984**, *106*, 4625. (b) Obara, S.; Koga, N.; Morokuma, K. *J. Organomet. Chem.* **1984**, *270*, C33.
(4) (a) Dawoodi, Z.; Green, M. L. H.; Mtetwa, V. S. B.; Prout, K. *J. Chem. Soc., Chem. Commun.* **1982**, 802. (b) Dawoodi, Z.; Green, M. L. H.; Mtetwa, V. S. B.; Prout, K. *Ibid.* **1982**, 1410. (c) Green, M. L. H.; Williams, J. M., private communication.

0002-7863/85/1507-7109$01.50/0

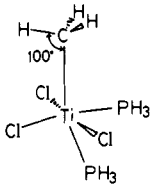

6

calculations demonstrate that the characteristic structural features that have been attributed to agostic interaction are indeed of electronic origin. The analysis of wave functions and orbitals suggests that the driving force of agostic interaction is the donative interaction from the CH bond to low-lying unoccupied Ti d orbitals.

Although examples of CH···M interaction in stable molecules have been accumulating rapidly as mentioned above, there exists no direct evidence for such an interaction playing a role in a chemical reaction. In this paper we report the results of ab initio MO calculation on the β-elimination reaction of the three-coordinate d^8 complex, $Pd(C_2H_5)(H)(PH_3)$ (**1**) and show that the

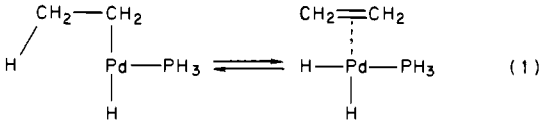

(1)

1 2

agostic interaction in fact plays an essential role in the β-elimination reaction. Most β-elimination reactions have been considered to proceed through the dissociation of a ligand and the formation of an open coordinate site.[6] The ethyl complex, **1**, has been chosen as the model complex of such an intermediate. It is well-known that β-elimination and its reverse insertion reaction often take place reversibly. However, when an ethyl group has electron-withdrawing substituents, the substituted ethyl complex becomes more stable than the corresponding ethylene hydride complex, and the reversibility of reaction is lost.[7] In order to reveal the origin of different behaviors, we will also examine CH···M interaction and β-elimination reaction of the difluoroethyl complex $Pd(CH_2CHF_2)(H)(PH_3)$ (**3**). Furthermore, we will carry out the investigation

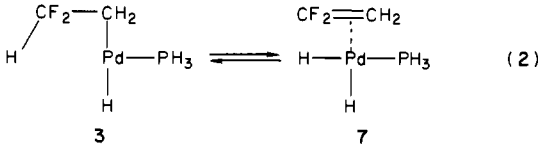

(2)

3 7

of $Ni(C_2H_5)(H)(PH_3)$ (**4**) in order to clarify the effect of a transition element on the structure and reactivity. The reverse

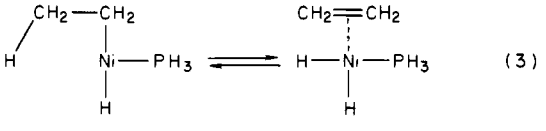

(3)

4 8

insertion reaction is known to be an important elementary reaction for the formation of an MC bond from an MH bond and olefin. Therefore, we will also examine insertion reactions for all three model systems.

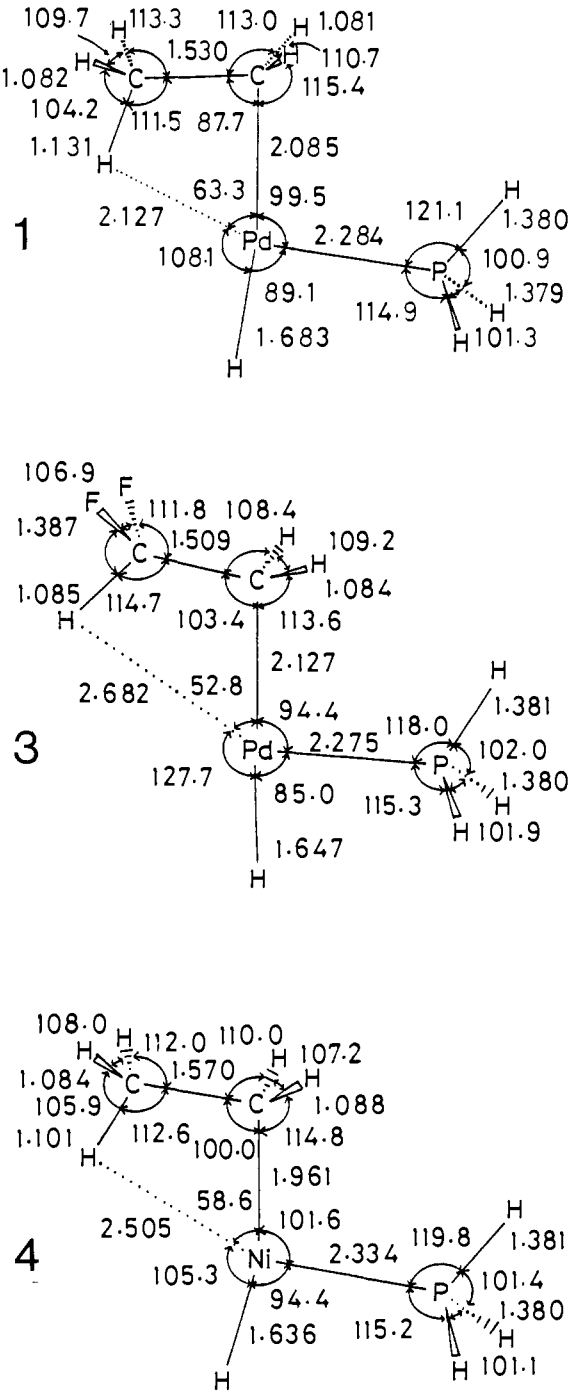

Figure 1. Optimized geometries of $Pd(C_2H_5)(H)(PH_3)$ (**1**), $Pd(CH_2CHF_2)(H)(PH_3)$ (**3**), and $Ni(C_2H_5)(H)(PH_3)$ (**4**). The bond distances are in angstroms and the angles in degrees.

Methods of Calculations

The ab initio closed-shell Hartree–Fock (HF) method with the energy gradient technique was used for the geometry optimization.[8] The fully optimized geometries of stable complexes (reactant and product) and the transition state for each model reaction system have been obtained. Throughout the reaction the systems have been assumed to retain C_s symmetry. For reaction 1, the frozen core second-order Møller–Plesset perturbation (MP2) calculation was carried out at the HF optimized geometries to obtain better energetics. For Pd and Ni, valence double-ζ basis functions of

(5) In a related subject, $Ti(CH_3)(Cl)_3$ has been calculated to have a C_{3v} symmetry with a flatted methyl group with a Ti–C–H angle of 107.5°,[5a] while an electron diffraction study has given a similar C_{3v} structure with the corresponding angle of 104°.[5b] (a) Koga, N.; Morokuma, K., unpublished results. (b) Green, M. L. H., private communication.

(6) Kochi, J. K. "Organometallic Mechanisms and Catalysis"; Academic Press: New York, 1978; p 246.

(7) (a) Clark, H. C. *J. Organomet. Chem.* **1980**, *200*, 63. (b) Clark, H. C.; Jablonski, C. R.; Wong, C. S. *Inorg. Chem.* **1975**, *14*, 1332. (c) Clark, H. C.; Jablonski, C. R.; Halpern, J.; Mantorani, A.; Weil, T. A. *Inorg. Chem.* **1971**, *13*, 1541. (d) Yagupsky, G.; Brown, C. K.; Wilkinson, G. *J. Chem. Soc., Chem. Commun.* **1969**, 1244.

(8) All the calculations were carried out with the GAUSSIAN80 program: Binkley, J. S.; Whiteside, R. A.; Krishnan, R.; Seeger, R.; DeFrees, D. J.; Schlegel, H. B.; Topiol, S. Kahn, L. R.; Pople, J. A. Program 406 in Quantum Chemistry Program Exchange Catalogue 13 (Indiana University, Bloomington, 1981).

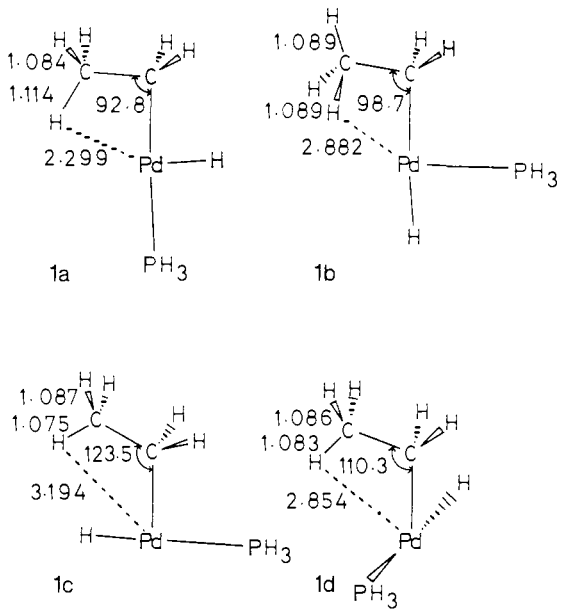

Figure 2. Optimized geometries of isomers of **1**. The bond distances are in angstroms and the angles in degrees.

Hay[9a] and Hay and Wadt[9b] were used, respectively, together with the core basis functions of MINI-1 of Tatewaki et al.[10] The 3-21G basis set is used for C and H of C_2H_5 and F and the STO-2G for P and H of PH_3.[11]

Results and Discussion

Agostic Interaction in Ethyl Complexes. In Figure 1 we show the optimized geometries of our model ethyl complexes, **1**, **3**, and **4**. It is noted that there are three unusual features in the structure of **1**. The distance between the H^β of the ethyl group and the Pd atom is short, 2.13 Å. The CH^β distance of 1.13 Å is longer by 0.05 Å than that of the other CH bonds in the same ethyl group. The Pd–C–C bond angle is 88°, much smaller than that expected in the sp^3 hybridization (109°). All these features point to the existence of direct CH^β···Pd agostic interaction. One also notes that these structural features of the ethyl group in this palladium complex are very similar to what have been found, experimentally and theoretically, in the titanium–ethyl complex.

In order to shed light on the nature of the agostic interaction, we have also optimized the geometries of isomers of **1**, as shown in Figure 2. A distorted structure has been obtained for the isomer **1a** in which PH_3 is trans to the ethyl group. The extent of ethyl distortion, a measure of the strength of agostic interaction, is less in **1a** than in **1**, indicating a larger trans influence of the hydride ligand than the phosphine. When the ethyl group is forced to have a staggered conformation, **1b**, the Pd–C–C angle is 98° with the H^β···Pd distance of 2.88 Å, indicating even a weaker interaction. The energy of **1b** is higher than that of **1** by 0.4 kcal/mol, and assuming 2.9 kcal/mol as the rotation barrier of the ethyl group, one can estimate the lower limit of the CH^β···Pd interaction energy in **1** to be 3.3 kcal/mol.

A drastically different result has been obtained for the isomer **1c** where both H and PH_3 are cis to the ethyl group. The geometry optimization gave a normal, undistorted ethyl group with a long H^β···Pd distance of 3.2 Å. The ethyl group was found to be normal and undistorted, even when it was allowed to approach Pd from the apical direction (**1d**). One also notes that the optimized geometry of the four-coordinate *trans*-$Pd(C_2H_5)(H)(PH_3)_2$ (**9**) has a normal, undistorted ethyl group.

(9) (a) Hay, P. J. *J. Am. Chem. Soc.* **1981**, *103*, 1390. (b) Hay, P. J.; Wadt, W. R. *J. Chem. Phys.* **1985**, *82*, 270.
(10) (a) Sakai, Y.; Tatewaki, H.; Huzinaga, S. *J. Comput. Chem.* **1982**, *3*, 6. (b) Tatewaki, H.; Huzinaga, S. *J. Chem. Phys.* **1979**, *71*, 4339.
(11) (a) Binkley, J. S.; Pople, J. A.; Hehre, W. J. *J. Am. Chem. Soc.* **1980**, *102*, 939. (b) Hehre, W. J.; Stewart, R. F.; Pople, J. A. *J. Chem. Phys.* **1969**, *51*, 2657.

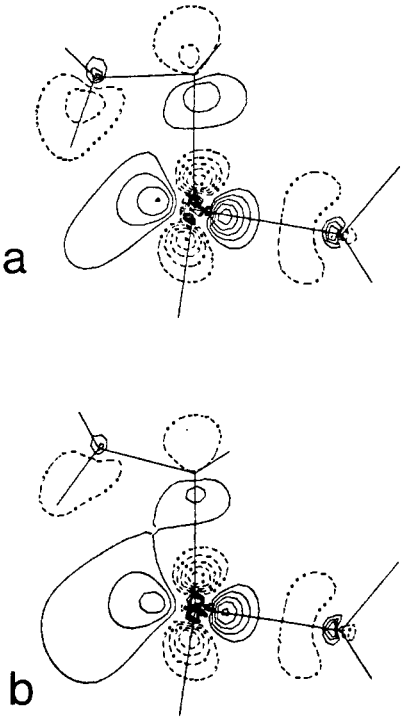

Figure 3. Contour maps of LUMO of **1** (a) at the optimized geometry and (b) at a geometry in which the M–C–C angle and the CH^β distance are assumed to be 105° and 1.081 Å, respectively, while the other geometrical parameters are kept at the values in part a. The contours are ±0.05, ±0.10, ±0.15, ±0.20, ±0.25, and ±0.30 au, and solid and dotted lines denote positive and negative values, respectively.

We can deduce from these results that the availability of an empty site next to the ethyl group is definitely a critical factor favoring a direct CH···M interaction in this system. The lowest unoccupied molecular orbital (LUMO) of **1** and its isomers extends around the empty site of the Pd atom, and thus the donative interaction, **10**, seems to be in operation in **1** as in **5**. We show

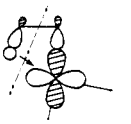

10

in Figure 3 the LUMO of **1** (a) at the optimized structure, **1**, and (b) in an assumed structure, **11**, with the Pd–C–C angle of 105° and the CH^β distance of 1.081 Å in which the CH^β···M interaction presumably is not taking place. The LUMO at the optimized

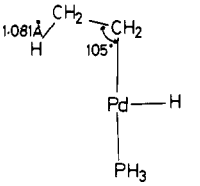

11

structure is higher in energy than at the assumed noninteracting structure and includes a larger $CH\sigma$ component in the antibonding manner, indicating the existence of the interaction between CH σ and d orbitals. It is also found that p_x mixes with $d_{x^2-y^2}$ in the LUMO in such a way that the LUMO extends toward the direction of H^β. The difference between the donative interaction of **5** and that of **1** is that in the former the acceptor orbital is d_{xy} and in the latter its main component is $d_{x^2-y^2}$, as d_{xy} is filled.[3a] The CH^β distance of **1** is longer by 0.02 Å than that of **5**, showing that the agostic interaction in **1** is stronger than in **5**, despite the smaller electron deficiency in **5** (formal electron count = 14) than in **1** (formal electron count = 12). This indicates that the availability

of an empty site favors more strongly the agostic interaction than the electron deficiency does.

Another structural feature of **1** is a short CC bond length of 1.53 Å, suggesting that the CC bond has a small extent of double bond character ascribed to interaction **10**, in which orbitals on the carbon atoms interact in phase with each other.

Although the difluoroethyl group in **3** and the ethyl group in **4** are not as distorted as the ethyl group in **1**, the M–C–C angles are still smaller than 109°, suggesting that **3** and **4** have a weak agostic interaction. The CH^{β} bond length in **3** is 1.08 Å and the Pd–C–C angle is 103°. Since the electron-withdrawing fluorines on the β-carbon atom make the electron-donating ability of the CH bond weaker, the CH···M interaction is not as strong as in **1**. **4** also has a structure like **3** with the Ni–C–C angle of 100°. The energy of the vacant d orbital in this Ni complex (0.1069 hartree) is higher than that (0.0505 hartree) in the Pd complex, **3**, and the Ni d orbital is tighter and has a smaller overlap with $CH\sigma$ than the Pd d orbital. Consequently, the donative interaction is weaker in the Ni complex. These results support the conclusion that the origin of the agostic interaction is the donative interaction from the CH σ bond to the empty metal d orbital. Comparing **3** and **4**, one finds that the CH^{β} bond length in **4**, 1.10 Å, is slightly longer than that in **3**, and the M–C–C angle in **4** is slightly smaller than that in **3**, implying that the CH···M interaction in **4** is a little stronger than that in **3**.

General Guideline for Existence of Agostic Interaction. From our studies on Ti and Pd complexes mentioned above, we may deduce a general guideline favoring the agostic interaction.

(1) Donative Interaction from the CH^{β} σ Bond to the Low Energy Metal Vacant Orbital. For an early transition metal this is rather easily accomplished. For a second and third row late transition metal an open coordination site next to the alkyl group creates this situation. For a first row late transition metal an agostic interaction may be difficult. A ligand with a strong trans influence will disfavor the agostic interaction.

(2) Weak Repulsion between the CH^{β} Bond and Metal. It is well-known that the interaction between occupied orbitals is repulsive. The lack of d electrons in the direction of the CH^{β} bond favors an agostic interaction.

(3) Additional Stability. The double-bond character of the CC bond as the result of agostic interaction, as was found in Pd complexes, stabilizes the complex.

β-Elimination and Insertion Reactions. The optimized structures of the β-elimination reaction products, **2**, $Pd(H)_2(CH_2CF_2)(PH_3)$ (**7**), and $Ni(H)_2(C_2H_4)(PH_3)$ (**8**), are shown in Figure 4. The CC bond distances of all the ethylene complexes are nearly as short as that of a free ethylene, and the distances between ethylene and the central metal are long. As was shown previously,[9a,12a] in planar ethylene complexes, ethylene weakly attaches to the central metal. Although the upright structures are more stable,[9a,12] the planar structure can be considered to be the direct product of the β-elimination reaction.

In Figure 5 we show the transition state connecting ethyl and ethylene complexes via β-elimination and its reverse, insertion reaction. In the β-elimination reaction, the hydrogen transfers from the β-carbon atom to the empty site of the metal atom. At the transition state of **1**, the distance between the Pd atom and the hydride is 1.64 Å, longer by only 0.02 Å than the other PdH distance, and the CC bond length of 1.40 Å is closer to that of **2** than that of **1**. These results indicate that the transition state of the β-elimination reaction is located "late". On the other hand, the PdC^{α} length is not so long as that of **2**, and the distance between the Pd atom and the β-carbon of 2.365 Å is short, showing that the transition state is "tight" as well.

At the transition state of the difluoroethyl complex, **3**, the CH^{β} length is longer than that of **1**; the transition state of **3** is located slightly later than that of **1**. On the other hand, the structure of the transition state of **4** is very different from those of **1** and **3**;

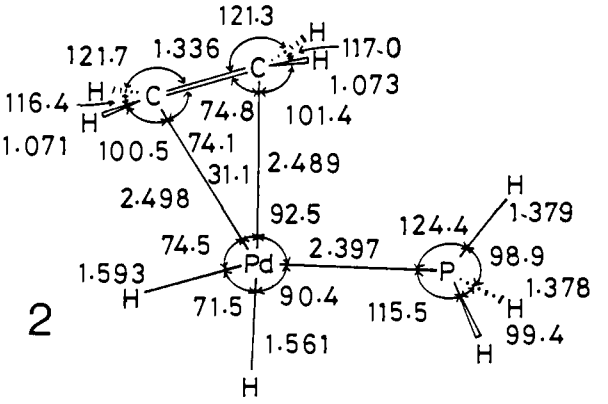

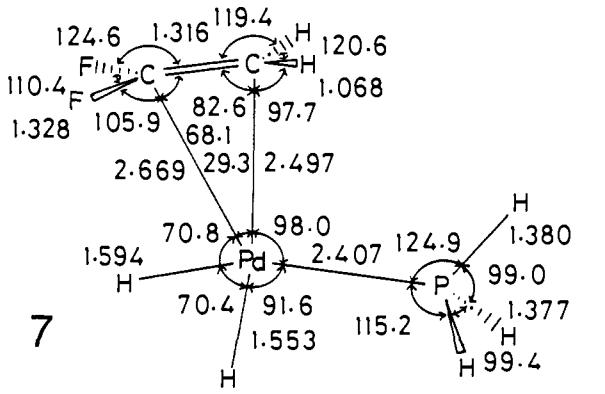

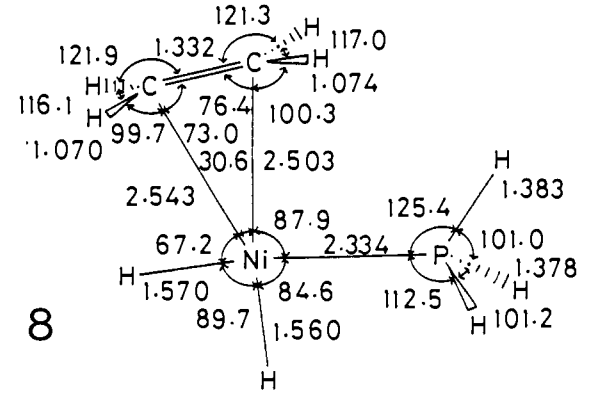

Figure 4. Optimized geometries of $Pd(H)_2(C_2H_4)(PH_3)$ (**2**), $Pd(H)_2(CH_2CF_2)(PH_3)$ (**7**), and $Ni(H)_2(C_2H_4)(PH_3)$ (**8**). The bond distances are in angstroms and the angles in degrees.

the $C^{\beta}H$ distance is very long, and the CC distance and the NiH distance are very short, compared with those of **1** and **3**. The transition state is located extremely late and very close to that of **8**.

These structural features are reflected in the energy profiles of reactions. In Table I we show the relative energies of **1**, **2**, and the transition state between them with the HF and the MP2 method and those for **3** and **4** with the HF method, calculated at the HF optimized geometries. The energy barriers for the β-elimination and the insertion reactions of **1** are 11.0 and 8.0 kcal/mol, respectively, with the HF method, and become even lower when the electron correlation is taken into account. Even at the MP2 level of calculation, the absolute value of barrier height may contain errors up to several kcal/mol, though the comparison between different systems may be more reliable. The low-energy

(12) (a) Bäckvall, J.-E.; Björkman, E. E.; Pettersson, L.; Siegbahn, P. *J. Am. Chem. Soc.* **1984**, *106*, 4369. (b) Albright, T. A.; Hoffmann, R.; Thibeault, J. C.; Thorn, D. L. *J. Am. Chem. Soc.* **1979**, *101*, 3801.

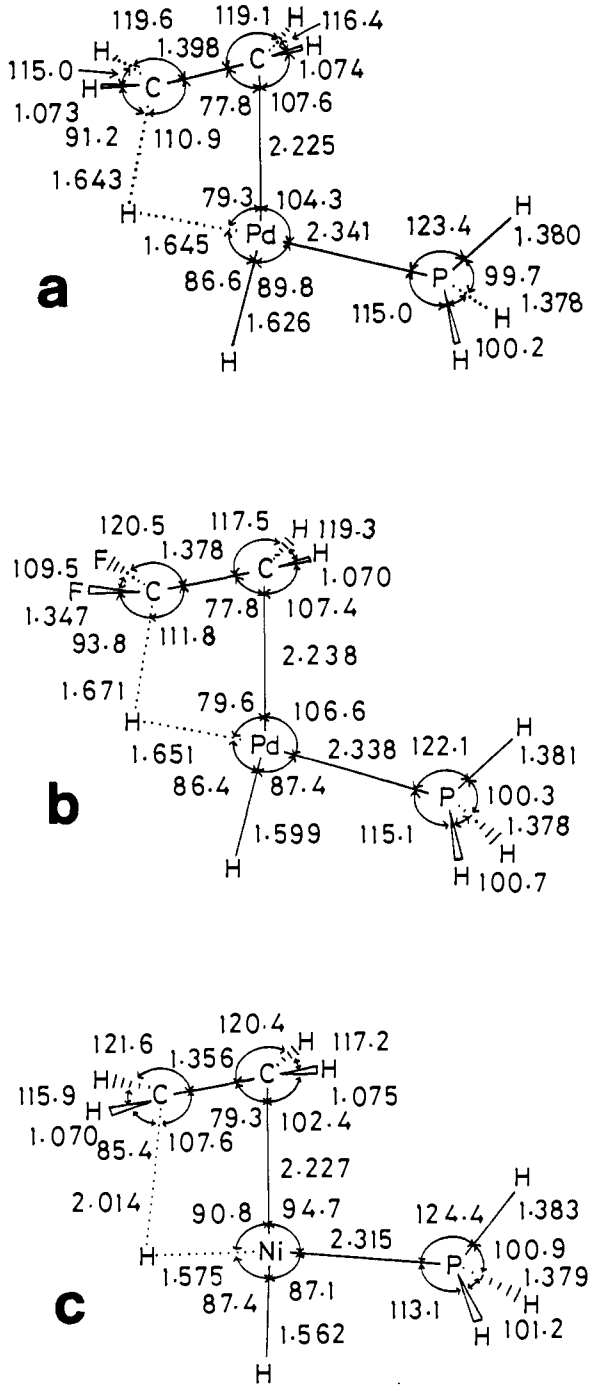

Figure 5. Optimized structures of transition states between (a) **1** and **2**, (b) **3** and **7**, and (c) **4** and **8**. The bond distances are in angstroms and the angles in degrees.

Table I. Relative Energies (in kcal/mol) for $M(CH_2CHX_2)(H)(PH_3) \rightleftarrows M(H)_2(C_2X_2H_2)(PH_3)$ (M = Pd, Ni; X = H, F)

M	X	ethyl complex	transition state	ethylene complex
Pd	H	0.0	11.0	3.0
		0.0[a]	2.1[a]	−3.0[a]
Pd	F	0.0	18.4	11.1
Ni	H	0.0	32.1	31.5

[a] The results obtained with the MP2 method, calculated at the HF optimized geometries.

barriers for both directions point to the reversibility of β-elimination and insertion reactions. An equilibrium between the ethyl complex and the ethylene complex has been observed experimentally in some complexes.[13] While the energy barrier for the reverse insertion reaction **7** → **3** is comparable to that of **2** → **1**, the barrier for β-elimination reaction **3** → **7** is higher by 7.4 kcal/mol than that of **1** → **2**, consistent with the above finding that the former transition state is later than the latter. The lower β-elimination barrier for **1** that has an agostic interaction than for **3** that has little interaction suggests that the barrier and the interaction are closely related. It looks as though the agostic interaction has incipiently activated the CH^{β} bond in the reactant, and therefore the reactant **1** requires less energy to break the bond.

For the Ni complex **4**, despite of a weak CH···M interaction, the energy barrier is the highest among three systems. Therefore, the facile β-elimination reaction is controlled not only by a CH···M interaction accompanying the formation of an open coordinate site but also by properties of the central atom. We will address this problem later. The activation energy for insertion reaction of the nickel complex is very low; in a better calculation the ethylene complex may not even be a stable species. In either case, the reversibility is lost and the equilibrium should be shifted toward the ethyl complex.

Though the β-elimination/insertion equilibrium is known to take place easily, the only available experimental data for the activation enthalpy is 13.0 kcal/mol obtained by the magnetization-transfer technique for the insertion reaction of a Rh complex.[14,15] Our theoretical values of Pd complexes are not far from

$$cis\text{-}Rh(H)(C_2H_4)(P\text{-}i\text{-}Pr_3)_2 \rightleftarrows Rh(C_2H_5)(P\text{-}i\text{-}Pr_3)_2 \quad (4)$$

it. In a d^8 ethyl complex with an open coordination site formed as a result of insertion reaction, it would be easy for CH···M interaction to take place. Therefore, we predict that $Rh(C_2H_5)(P\text{-}i\text{-}Pr_3)_2$, if isolated, would have a distorted ethyl group. Thorn and Hoffmann's conclusion based on a qualitative analysis of molecular orbitals that the cis insertion reaction via a 4-coordinate d^8 metal complex occurs with a small barrier is supported by our result.[16]

There has been a general interest on how the insertion reaction takes place, via ethylene insertion into an MH bond or hydrogen migration from metal to a ethylene carbon. For the insertion reaction of **2**, the former mechanism will give **1e**, while the latter will result in **1**. Though we have not followed the path from the

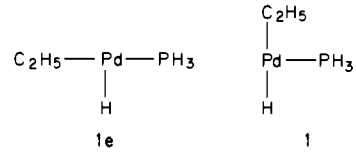

transition state (Figure 5a) to the insertion product, the transition-state structure suggests that the product is more likely to be **1**, supporting the hydrogen-migration mechanism.

Orbital Mixing in the β-Elimination Reaction. Hereafter, we present a qualitative argument of orbital interaction and resulting electronic structure changes, justifying the calculated results for the β-elimination reaction. The argument is based on orbitals in an ethyl complex without agostic interaction and their mixing during the course of agostic interaction and reaction. The basic orbitals we used are the bonding and antibonding orbitals of the CH^{β} bond, the CPd bonding orbital, the vacant metal orbital extending over the empty coordinate site, and the metal d_{xy} orbital, represented as σ_{CH}, σ_{CH}^*, σ_{CPd}, σ_v^*, and d_{xy}, respectively, in the first row of Scheme I. Though these orbitals are rather conceptual and do not correspond to individual HF canonical orbitals, one can identify some of them among HF canonical orbitals and their linear combinations. For instance, σ_{CPd}, **14**, can be considered

(13) (a) Byrne, J. W.; Blaser, H. U.; Osborn, J. A. *J. Am. Chem. Soc.* **1975**, *97*, 3871. (b) Werner, H.; Feser, R. *Angew. Chem., Int. Ed. Engl.* **1979**, *18*, 157.

(14) Roe, D. C. *J. Am. Chem. Soc.* **1983**, *105*, 7770.

(15) More recently, Miller and Grant have obtained an activation energy of 9.4 kcal/mol for the hydrogenation of ethylene by $Fe(CO)_4(C_2H_4)$ where the rate-determining step has been considered to be ethylene insertion into the Fe–H bond. The activation energy is close to that presently obtained. Miller, E. R.; Grant, E. R. *J. Am. Chem. Soc.* **1985**, *107*, 7770.

(16) Thorn, D. L.; Hoffmann, R. *J. Am. Chem. Soc.* **1978**, *100*, 2079.

Scheme I

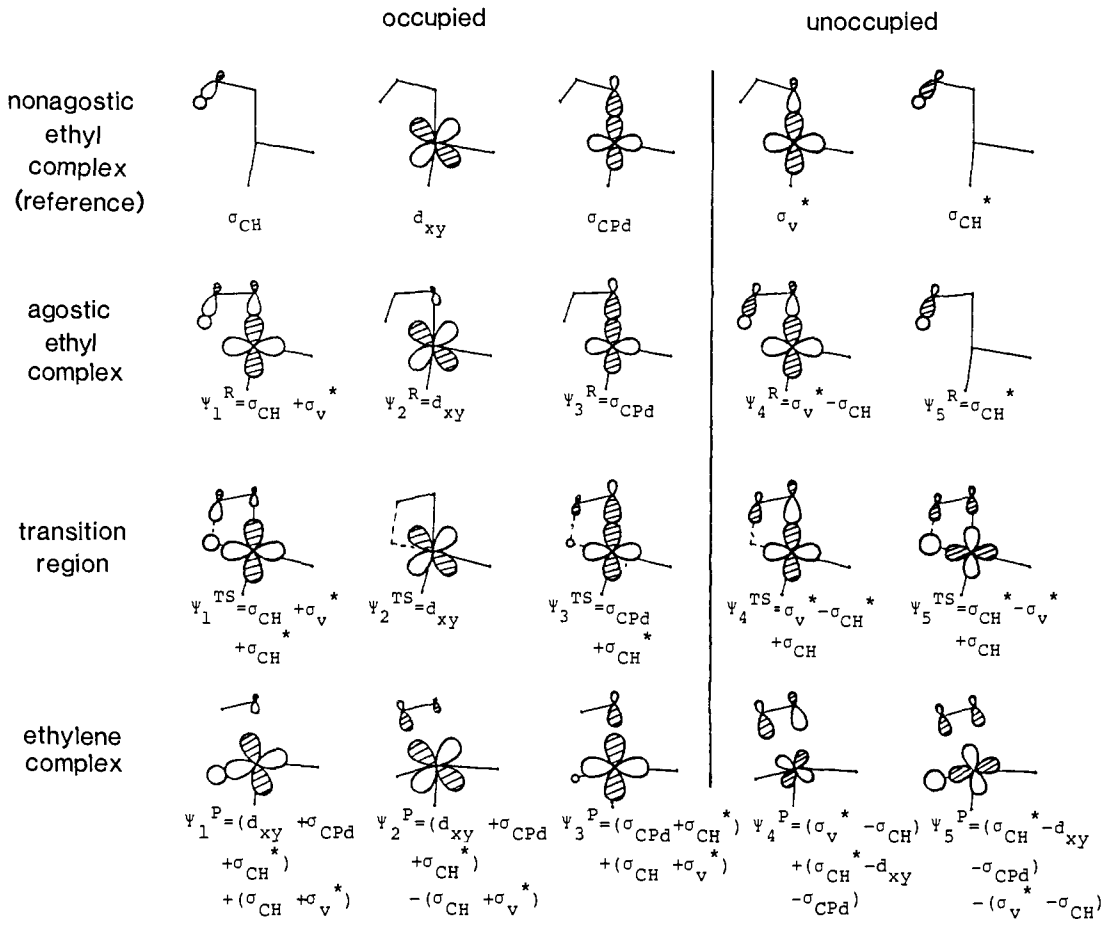

to be a linear combination of two occupied canonical orbitals, **12** and **13**.

12 **13** **14**($=\sigma_{CPd}$)

Actually, in the nonagostic Pd complex, **11**, as shown in Figure 6, the HF canonical orbitals 28a′ and 30a′ (HOMO) correspond to **12** and **13**, respectively. The orbital 31a′ (LUMO) of **11** corresponds to σ_v^*, carrying an antibonding character between Pd and C^α. Characters of σ_{CH} and σ_{CH}^* can be observed in several occupied and vacant canonical orbitals, which are heavy mixtures of σ_{CH}, σ_{CH}^*, CC bond orbitals and metal d orbitals. The d_{xy} orbital is a well-defined lone-pair orbital, 27a′.

Now, let us consider mixing of these five orbitals during the agostic interaction and the β-elimination reaction of Pd complexes. In Scheme I, we show schematically the molecular orbitals constructed as admixtures of σ_{CH}, σ_{CH}^*, σ_v^*, σ_{CPd} and d_{xy}, at the agostic ethyl complex and the ethylene complex and in the transition region, a region around the transition state. When the ethyl group is agostic, σ_{CH} and σ_v^* mix with each other, representing the donative interaction from the CHσ bond to a d orbital of the Pd atom. In addition, the CC bond has a small amount of double bond character due to the in-phase mixing of carbon orbitals in σ_{CH} and σ_v^*, and the PdC^α bond weakens due to contribution of σ_v^*.[17]

As the system enters the transition region where the electronic reorganization takes place, σ_{CH} interacts with σ_v^* more strongly. In addition, σ_{CH}^* mixes in, due to its lowering energy and increased overlap with σ_v^*, Ψ_1^{TS}, the result of these orbital interactions, is an admixture given in **15**. As a result, the PdH bond is just

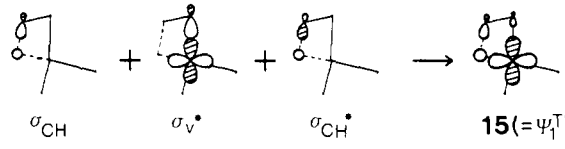

σ_{CH} σ_v^* σ_{CH}^* **15**($=\Psi_1^{TS}$)

being formed and the CH^β bond being broken. One finds that Ψ_1^{TS} actually can be represented as a linear combination of two HF canonical orbitals, in the same way as **14**. In Ψ_3^{TS} σ_{CH}^* slightly mixes in with σ_{CPd}. d_{xy} more or less keeps its original character.

In the second half of the reaction, proceeding from the transition region to the ethylene complex, the electronic structure goes through another stage of changes. The participation of σ_{CPd} and d_{xy} in the interaction with σ_{CH}^* is its key ingredient. As Ψ_1^{TS} changes to Ψ_1^P, the in-phase combination of donative interaction $\sigma_{CH} + \sigma_v^*$ and back-donative interaction ($\sigma_{CPd} + d_{xy}$) + σ_{CH}^* results in cleavage of the CH bond and formation of the PdH bond as given in **16**. The out-of-phase combination Ψ_2^P as well as Ψ_3^P

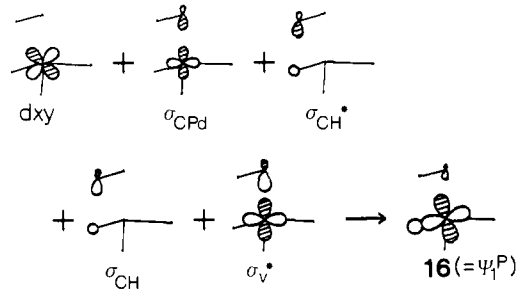

dxy σ_{CPd} σ_{CH}^*

σ_{CH} σ_v^* **16**($=\Psi_1^P$)

can be regarded as the results of linear combination of **17** and

(17) Since the vacant orbital of the Ti–ethyl complex **5** has no antibonding character between Ti and C^α,[3a] the weakening of the TiC^α bond does not take place. Therefore, β-elimination does not occur.

(18) Note also that for d^8s^2 Ni and Pd atoms the d orbital energies are −0.71 and −0.66 hartree, respectively, and the radii of maximum charge density are 0.33 and 0.55 Å, respectively. For d^8 Ni(II) and Pd(II), the orbital energies are −1.42 and −1.28 hartree, respectively: Fraga, S.; Saxena, K. M. S.; Karwowski, J. "Handbook of Atomic Data"; Elsevier: Amsterdam, 1976.

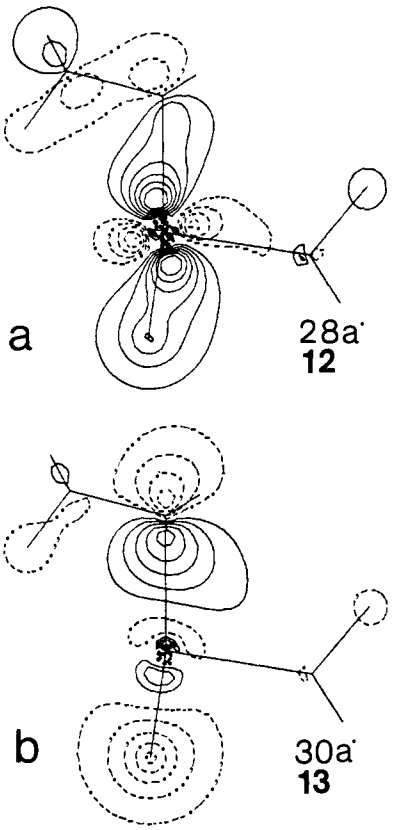

Figure 6. Contour maps of (a) MO 28a′ and (b) MO 30a′ of **11**. The contours are ±0.05, ±0.10, ±0.15, ±0.20, ±0.25, and ±0.30 au, and solid and dotted lines denote positive and negative values, respectively.

18 which represent the donation and back-donation between ethylene and the transition metal. They suggest that to some extent **2** has a character of metallacyclopropane.

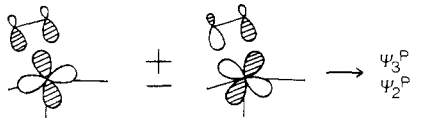

17 **18**

The above argument, therefore, suggests that the β-elimination reaction can be regarded as a $[2_s + 2_s]$ reaction. Formation of the PdH bond and the CC double bond, cleavage of the CH^{β} bond, and weakening of the PdC^{α} σ bond all occur concertedly. Since both σ_{CH} and σ_{CH}* can overlap with σ_v* and σ_{CPd}, respectively, as mentioned above, this $[2_s + 2_s]$ reaction is regarded as allowed. The interaction between d_{xy} and σ_{CH}* does not contribute to the bond exchange but gives rise to the additional product stabilization, the back-donation between ethylene, and the transition metal.

On the basis of the above considerations, it is found to be important in the β-elimination reaction that in an early stage of reaction a CH···M interaction takes place, whose origin is the electron-donative interaction from a CH σ bond to a vacant d orbital and that in a late stage of reaction the electron is donated back from an occupied d orbital and the PdC bond orbital to the CH σ* orbital.

While the β-elimination reaction of a complex without the agostic ethyl group starts with σ_{CH}, that of a complex with the agostic ethyl group starts with Ψ_1^R, a partially activated orbital. This difference accounts for an incipient CH activation in **1**. Obviously, in the β-elimination of the difluoroethyl complex, the interaction between σ_{CH} and σ_v* is weakened by the decrease of electron-donating ability of σ_{CH}, leading to a higher activation energy.

The process for reaction of the Ni complex is different from that of Pd complexes. One factor is that the d_{xy} lone-pair orbital in Ni complexes is lower in energy and tighter in distribution than

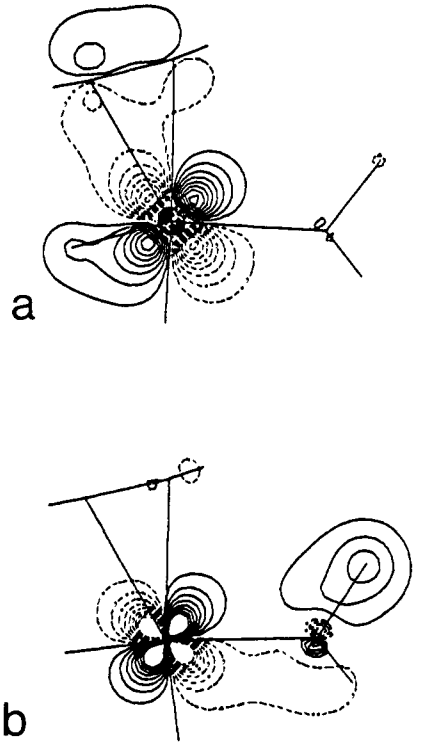

Figure 7. Contour maps of (a) MO 27a′ of **2** and (b) MO 18a′ of **8**. The contours are ±0.05, ±0.10, ±0.15, ±0.20, ±0.25, and ±0.30 au, and solid and dotted lines denote positive and negative values, respectively.

in Pd complexes. For instance, the MO 18a′ of **8** has an energy of −0.5759 hartree and a contour map shown in Figure 7b, while the MO 27a′ of **2** has a higher energy of −0.4354 hartree and a more spread-out contour map shown in Figure 7a.[18] The situation is similar in ethyl complexes as well as at the transition state. Therefore, the Ni d_{xy} lone pair does not interact strongly with the orbitals of the ethyl group throughout the reaction. Even in the ethylene complex, one sees little back-donation, as in Figure 7b. The second and similarly important factor is that the d character of the NiC bonding orbital is smaller than that of σ_{CPd}. In the later stage of reaction, σ_{CPd} can interact effectively with σ_{CH}* as the positive and the negative lobe of σ_{CPd} overlap nicely with the respective lobe of σ_{CH}* (**19a**). In the Ni complex, however, the large positive lobe of σ_{CNi} cannot overlap nicely with the σ_{CH}* (**19b**). Due to these two factors, σ_{CH}*, which mixes into σ_{CH}

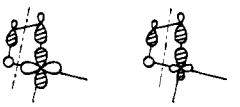

19a **19b**

through σ_{CPd} and d_{xy} in the Pd complexes, cannot considerably mix with σ_{CH} in the Ni complex, until σ_v*, instead of σ_{CPd} and d_{xy}, overlaps and comes into interaction with σ_{CH}*. As a result, the CH bond length of 2.014 Å at the transition state of **4** (Figure 5c) is longer. These two factors are probably the reasons why the energy barrier for β-elimination of **4** is much higher than those of both **1** and **3**.[19]

In the study for thermal decomposition of *cis*-$Co(C_2H_5)_2(acac)(PPhMe_2)_2$, the activation energy for the β-elimination is estimated to be about 31 kcal/mol,[20] not far from the calculated value of the Ni complex. The mechanism of β-elimination in this d^6 Co complex, having been found to occur after the dissociation of a ligand, is probably very similar to that of the present Ni

(19) The difference of reductive elimination between nickel complex and palladium complex has been discussed by Tatsumi et al. using extended Hückel orbital energies: Tatsumi, K.; Hoffmann, R.; Yamamoto, A.; Stille, J. K. *Bull. Chem. Soc. Jpn.* **1981**, *54*, 1857.

(20) Ikariya, T.; Yamamoto, A. *J. Organomet. Chem.* **1976**, *120*, 257.

complex,[21] as the extra vacant $d_{y^2-z^2}$ in the former is not heavily involved in the interaction mentioned above.

The protection of the vacant site with additional ligands is one of the ways to stabilize alkyl complexes by interrupting the path for decomposition via β-elimination.[22] The present result suggests a way of electronic stabilization, i.e., the interception of the interaction between σ_{CH} and σ_v^*, which is achieved by the reduction of electron-donative ability of the CH σ bond and/or electron-accepting ability of the central metal. An example of the former is the case of **3** and that of the latter is the case of **4**. In addition to them, it is also effective that the carbon metal bond has a smaller d character and the d lone pair orbital is lower in energy as in **4**.

Orbital Mixing in the Insertion Reaction. Next, we consider the insertion reaction. We follow the process in the reverse direction of β-elimination. In order to make Ψ_1^{TS}, **20**, using the orbitals of ethylene complex as new basic orbitals, it is necessarily that Ψ_1^P mix with Ψ_4^P and Ψ_2^P.

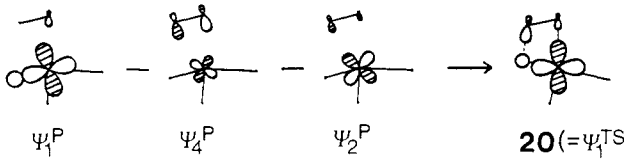

Especially, the mixing of occupied Ψ_1^P and unoccupied Ψ_4^P is important. This leads to weakening of the PdH and the PdC^β bond, decrease in the double bond character of the CC bond, and formation of the CH bond. Since the situations of the ethyl complex and the difluoroethyl complex are more or less the same, their activation energies are similar to each other.

The energy barrier for the insertion reaction of the nickel complex **8** is lower than those of **2** and **7**. While Ψ_4^P of **2** and **7** is an antibonding combination of ethylene π^* and metal d orbital, the low-lying Ni d orbital of **8** does not interact strongly with the ethylene π^* orbital, and therefore in the Ni complex π^* plays a role of Ψ_4^P of the Pd complexes. Since π^* is lower in energy than Ψ_4^P, the interaction between Ψ_1^P and π^* occurs easily, giving a low barrier.

The importance of the ethylene π^* orbital in the insertion reaction has been pointed out by several investigators.[12a,16,23] They have divided the system into ethylene and the metal fragment or ethylene, the hydride, and the remaining part and have discussed how the total interacting system is stabilized and new bonds are formed by the participation of π^*. Our views are different from theirs in that we use orbitals of the ethylene complex which in turn are represented by orbitals of the ethyl complex. By use of these orbitals and following the process in the reverse direction of β-elimination, we can show more clearly important orbital interactions describing the bond exchange during the reaction.

If the central metal is a high valent early transition metal in which d_{xy} is empty, the MH σ bond can interact with the bonding combination of ethylene π^* and metal d_{xy}, whose energy is expected to be lower, and thus the situation would be favorable for the insertion reaction. The mechanism is just the Cossee mechanism of the Ziegler–Natta catalysis.[24,25]

Conclusions

We optimized the geometries of coordinatively unsaturated $Pd(C_2H_5)(H)(PH_3)$, its β-elimination product $Pd(H)_2(C_2H_4)(PH_3)$, and the transition state connecting them as well as those of $Pd(CH_2CHF_2)(H)(PH_3)$ and $Ni(C_2H_5)(H)(PH_3)$ by means of the ab initio MO method with the energy gradient technique. It has been found that $Pd(C_2H_5)(H)(PH_3)$ has an agostic ethyl group, of which the CH σ bond interacts strongly with a vacant d orbital of the Pd atom. Its driving force is the electron-donative interaction from the former to the latter. In the difluoroethyl Pd complex, fluorine atoms prevent the interaction from occurring by weakening of the electron-donating ability of the CH σ bond. In the Ni complex the vacant d orbital is higher in energy and has a smaller overlap with CH σ than in the Pd complex, and thus a small agostic interaction is found. The low activation energy for the β-elimination reaction of $Pd(C_2H_5)(H)(PH_3)$ found in this study is ascribed to two factors: the CH σ bond has been incipiently activated due to the agostic interaction, and σ_{CPd} and the occupied d_{xy} orbital interact with σ_{CH}^* easily in the later stage of reaction.

In the reverse, insertion reaction, the Ni complex has a lowest barrier. The interaction between the MH bond orbital and the vacant orbital ethylene π^* orbital takes place more easily in the Ni complex than in Pd complexes.

Although it may not be easy to detect experimentally, the present study strongly suggests that in reactive intermediates an agostic interaction may be taking place more commonly than has been suspected.

Acknowledgment. The authors are grateful to Professors Sei Ohtsuka, Akio Yamamoto, and M. L. H. Green for stimulating discussions and suggestions. They also thank Dr. P. J. Hay for sending a preprint of ref 8b before publication. Numerical calculations were carried out at the Computer Center of the Institute for Molecular Science.

Registry No. 1, 98778-64-4; **2**, 98778-65-5; **3**, 98778-66-6; **4**, 98778-68-8; **7**, 98778-67-7; **8**, 98778-69-9.

(21) For the d^7s^2 Co atom, the d orbital energy is −0.68 hartree and the radius of maximum charge density is 0.35 Å,[18] close to those of Ni atom.

(22) Cotton, F. A.; Wilkinson, G. "Advanced Inorganic Chemistry"; Wiley: New York, 1980; p 1119.

(23) (a) Sakaki, S.; Kato, H.; Kanai, H.; Tarama, K. *Bull. Chem. Soc. Jpn.* **1975**, *48*, 813. (b) Fukui, K.; Inagaki, S. *J. Am. Chem. Soc.* **1975**, *97*, 4445. (c) Dedieu, A. *Inorg. Chem.* **1981**, *20*, 2803.

(24) (a) Cossee, P. *J. Catal.* **1964**, *3*, 80. (b) Cossee, P. *Recl. Trav. Chim. Pays-Bas* **1966**, *85*, 1151.

(25) The importance of π^* orbital in the model system of the Ziegler–Natta catalysis has also been pointed out by semiempirical and ab initio calculations: (a) Navaro, O.; Blaisten-Barojas, E.; Clementi, E.; Giunchi, G.; Ruiz-Vizcaya, M. E. *J. Chem. Phys.* **1978**, *68*, 2337. (b) Armstrong, D. R.; Perkins, P. G.; Stewart, J. J. P. *J. Chem. Soc., Dalton Trans.* **1972**, 1972.